Computer Methods in Applied Mechanics and Engineering 109 (1993) 1–15
North-Holland

Numerical investigation of the laminar boundary layer flow around an impulsively moved circular cylinder

C.I. Christov[1]

Servicio de Prediccion Numerica, Instituto National de Meteorologia, Calle de las Moreras s/n, Ciudad Universitaria, 28040 Madrid, Spain

I.T. Tzankov

Dept. of Fluid Mechanics, Institute of Mechanics, Institute of Mechanics and Biomechanics, Bulgarian Academy of Sciences, P.O. Box 373, Sofia, 1090, Bulgaria

Received 8 June 1990
Revised manuscript received 3 September 1992 and 13 January 1993

An implicit difference scheme of splitting type is developed for solving unsteady boundary layer equations with an unfavorable (adverse) pressure gradient. The results obtained compare quantitatively well with the results of Lagrangian numerical schemes and indicate that a singularity evolves after a finite time (approximately $t \to 3$ in dimensionless units).

Introduction

Since Prandtl introduced it, boundary layer approximation has turned out to be one of the most successful ideas of modern fluid mechanics because of its simplicity and practical significance. The main advantage of stationary boundary layer equations is that they are of parabolic type, with the longitudinal coordinate playing the role of a 'temporal' coordinate. The latter allows one to employ marching numerical procedures that are significantly less expensive in comparison with the methods for solving elliptic equations with an equivalent number of spatial coordinates.

The very nature of this advantage, however, turns out to be the cause for creating formidable obstacles in the way of applying the boundary layer approximation to separated steady flows where the longitudinal velocity component may become negative thus rendering the governing equations anti-parabolic and explosively unstable. This is the reason why the separated boundary layers were not exhaustively studied numerically.

The change of type of the boundary layer equations is not the only cause for deficiency when modelling separated flows. In fact, it is not of crucial importance for the unsteady separated boundary layers. The more dangerous problem is the occurrence of a singularity of the solution at the position of separation. This phenomenon was pointed out by Goldstein [1] and since then a unified point of view has not been reached on the question of whether boundary layer equations are applicable to reversed or separated flows with prescribed potential flow. One should not be deceived by the apparent success of the so-called schemes of viscous–inviscid interaction in which the 'outer' pressure gradient is adapted to the boundary layer through solving the potential problem with a prescribed influx on the rigid boundaries. This inflow is matched to the normal velocity at the edge of the boundary layer. The problem is that during the current iteration of the viscous–inviscid interaction, the mathematical

Correspondence to: Professor C.I. Christov, Servicio de Prediccion Numerica, Instituto Nacional de Meteorologia, Calle de las Moreras s/n, Ciudad Universitaria, 28040 Madrid, Spain.

[1] On leave from the National Institute of Meteorology & Hydrology, Bulgarian Academy of Sciences, Sofia 1184, Bulgaria.

problem is essentially the same as the above-mentioned problem for the boundary layer with prescribed (generally unfavorable) pressure gradient. The viscous–inviscid interaction in a sense hinders the problem because the unfavorable pressure gradients are 'milder'. However, should one stiffen the requirements for convergence of the 'inner' iteration (the iteration for the boundary layer velocity field) in the frame of the current 'outer' iterational stage of the viscous–inviscid interaction, one would inevitably discover that the inner iteration is not convergent to a steady solution because a singularity develops. The deceiving difference is that the singularity occurs after a much longer time and after a long period of apparent tendency to convergence. For this reason, we believe that the numerical problem of calculating the boundary layer under an unfavorable pressure gradient still deserves attention until consensus is reached on the issue of its mathematical properties. In addition, as we mention further, there is certain disagreement between the numerical results obtained in the Lagrangian and Eulerian frames. The purpose of the present work is to contribute to the Eulerian difference schemes for numerical solution of this problem.

The unsteady flow past an impulsively moving cylinder is one of the classical problems of dynamics of viscous fluids due to its practical importance, amenability to accurate experimental studies combined with relative simplicity, allowing one to employ various theoretical approaches, e.g., numerical integration of Navier–Stokes equations, method of matching asymptotic expansions, power series expansions with respect to time and/or harmonic series expansions. That is the reason why this flow serves as a test example for checking both the quality and performance of numerical schemes and the correctness of the different asymptotic approximations. For instance, in order to check the accuracy of their schemes for numerical solution of Navier–Stokes equations, Ta Phuoc Loc [2] and Ta Phuoc Loc and Bouard [3] compared the results obtained with the experimental results of Bouard and Coutanceau [4]. In turn, these numerical results fueled a prolonged discussion on the existence for arbitrary times of a smooth solution to the boundary layer equations with unfavorable pressure gradient. Refer to Telionis [5], Elliott et al. [6] and Cousteix [7] for comprehensive reviews on the subject.

One of the first numerical results concerning the developing boundary layer around an impulsively moving cylinder was published by Collins and Dennis [8]. They succeeded in finding a smooth solution up to dimensionless times as high as $t \to 2.5$. The last numerical value is compatible with the dimensionless variables employed in the present paper. Telionis and Tsahalis [9], however, found a smooth solution only up to $t = 1.3$. According to them, downstream of the point with zero skin friction, a singularity of the type of Goldstein [1] arises. Later, Cebeci [10] proposed another numerical technique and found a smooth solution for times up to $t \to 2.8$. He believed that the only reason for not proceeding beyond that value of time was the process of thickening of the boundary layer which decreased the numerical efficiency of his difference scheme. On this basis, he concluded that the solution exists for each finite time interval and no singularities develop that can prevent it from doing so. The latter contributed to continuing the controversy over the existence of singularity of solution of boundary layer equations.

The first accurate investigation, in the numerical sense, of the existence of a solution to the boundary layer equations up to the time of the singularity was performed by Van Dommelen and Shen [11]. They used a Lagrangian scheme and, unlike all the works cited above, verified it on a set of different grids with different spacing. Their results suggested that at a certain moment of time, a singularity is born that is not of the type of Goldstein singularity. For instance, the longitudinal distribution of tangential stress is not singular as it should be for a singularity of Goldstein's type. The singular behavior of the solution in their numerical experiments showed itself through a sharp increase in the amplitude of the longitudinal derivative of the velocity and of displacement thickness when $t \to 3$. The same authors [12] also proposed an asymptotic expansion for $t \to 3$, which compared very well with the numerical results.

The results of Van Dommelen and Shen were verified to a certain extent by other authors. Cebeci [13] repeated his computations and found that the results compared well with those of Van Dommelen and Shen [11] up to $t \to 2.75$. Although only qualitatively, the results of Wang [14] also support the notion of developing singularity. According to [14], singularity occurs at $t \to 2.8$. Employing the double series expansion approach of Collins and Dennis [8], Cowley [15] and Ingham [16] verified both the numerical and asymptotic results of [11] for $t \to 3$.

At the same time, Cebeci [17] is managed to give support to the opposite point of view and he

criticized the previous works (including his own) in the sense that the Courant–Friedrichs–Lewy condition had not been properly satisfied. Employing a new numerical procedure that apparently accounts for that condition, Cebeci [17] obtained a smooth solution up to $t \to 3.1$ and did not go further only because of the intolerable amount of computational time required.

Because of their nature, the conclusions of Cebeci [17] should have given rise to a wide discussion but in fact they did not mostly because the efforts were diverted to the more practical scheme of viscous–inviscid interaction. After [17], the problem was treated by Henkes and Veldman [18] and Riley and Vasanta [19] but mainly from the point of view of viscous–inviscid interaction. Concerning the limiting case of a non-interacting boundary layer, Henkes and Veldman [18] show that their numerical scheme gives results close to those of [11] but becomes unstable for $t \approx 2.8$. In the sense of stability, the results of Riley and Vasanta [19] are better. They employ stream function/vorticity formalism, but as is stressed in their work, the scheme does require a considerable amount of computational time because of the iterations (sometimes about 100) that were introduced everywhere a problem might arise. Thus they obtained reliable results in the Eulerian frame that are in very good agreement with those of [11, 15] in the frame of the Lagrangian approach.

In summary, it can be said that by means of significantly different numerical methods (Lagrangian and Fourier series), Van Dommelen and Shen [11], Ingham [16] and Cowley [15] have found that for an unsteady boundary layer at impulsively moving cylinder, a singularity develops in finite time. On the other hand, the results of Telionis and Tsahalis [9], Cebeci [10, 13, 17] and Wang [14] obtained by means of Eulerian difference schemes are not in concert neither among themselves nor with the results of the previous works. They do not clearly answer the question of whether singularity takes place or not.

In the present paper, another Eulerian scheme is proposed and the respective numerical algorithm is developed. It is an implicit splitting-type scheme which is unconditionally stable. All mandatory measures for securing good approximation are taken, e.g., non-uniform mesh spacings in the normal direction. A number of calculations with different magnitude of the longitudinal spacing are conducted in order to reveal the performance of the scheme in the vicinity of the separation point. The results obtained here are in good quantitative agreement with the results of the schemes of the first group [11, 15].

1. Posing the problem

Consider the two-dimensional viscous incompressible flow around a circular cylinder. Let U be the velocity of the flow at infinity, L the radius of cylinder, and ν the viscosity of the fluid. The natural way to render the velocities, spatial coordinate and time dimensionless is to scale them by U, L and L/U, respectively. Here, however, another set of scales, namely $2U$, L, $L/2U$ is also currently used [11, 13, 17]. For the sake of unification of the notation, the last set is used also in the present paper. For the normal coordinate y and normal component of velocity v, the scale factors $L/\mathrm{Re}^{0.5}$ and $2U/\mathrm{Re}^{0.5}$ are chosen, respectively. Here $\mathrm{Re} = 2UL/\nu$ is the Reynolds number. Finally, the governing equations in terms of dimensionless variables take the form

$$\frac{\partial u}{\partial x} + \frac{\partial v}{\partial y} = 0\,, \tag{1}$$

$$\frac{\partial u}{\partial t} + u\frac{\partial u}{\partial x} + v\frac{\partial u}{\partial y} = \frac{\partial U_e}{\partial t} + U_e\frac{\partial U_e}{\partial x} + \frac{\partial^2 u}{\partial y^2}\,, \tag{2}$$

where u and U_e are the longitudinal components of velocity in the boundary layer and in ideal flow, respectively. Equations (1) and (2) are coupled with the boundary and initial conditions. The boundary conditions at the cylinder surface read

$$u(t, x, 0) = v(t, x, 0) = 0\,, \tag{3}$$

and at the outer edge of the boundary layer,

$$u(t, x, y) \to U_e(t, x) \quad \text{for } y \to \infty . \tag{4}$$

The inlet condition ($x = 0$) corresponding to an impulsively moving cylinder is

$$u(t, 0, y) = 0 \quad \text{for } y = 0 , \qquad u(t, 0, y) = U_e \quad \text{for } y > 0 . \tag{5}$$

The equation of the unsteady boundary layer has two 'marching' coordinates, t and x, and require therefore 'initial' conditions also with respect to x. For this reason, alongside (5), one also needs an 'initial' (in fact a boundary) condition with respect to x. The zones of influence of the initial conditions must cover the entire region under consideration (see, e.g., [5]). When no separation or/and reversion is present, the problem is fully defined by the conditions at the leading end point (the 'inlet' condition). When the flow reverses at the rear end point one needs an 'initial' x-condition at that point. In the case under consideration, the required condition is a corollary of the symmetry. In terms of the adopted notation, it reads

$$u = 0 \quad \text{for } x = 0, \pi . \tag{6}$$

2. Coordinate transformation

From a numerical point of view, the most complicated part of the problem under consideration is the asymptotic boundary conditions (4) which must be satisfied in a finite interval of the transverse coordinate y. The boundary layer calculations are an inverse problem in which the thickness of the boundary layer is defined implicitly from an 'additional' condition on the normal derivative of the velocity at the edge of the layer. The inverse nature is the reason why the numerical treatment of the boundary layer flow is very sensitive to the particular implementation of the condition defining the thickness of the layer. Additional difficulties are created in separated layers by the highly non-uniform profile of the thickness as a function of the longitudinal coordinate. For instance, in the vicinity of the leading end point, the layer is all the time as thin as $\mathrm{Re}^{-0.5}$, while around the rear end point, its thickness grows with time to the order of unity [20, 21].

The problem of adjusting the computational boundaries remains crucial in the numerical treatment of boundary layer flows. For this reason, a number of different ideas have been employed. In earlier numerical works, the solution was sought in a large enough region, defined a priori in the plane (x, y) and the calculations were conducted until the boundary layer grew beyond the chosen frame [10]. In certain algorithms, the fixed computational domain is 'updated' at a certain moment by adding new grid points [9]. Unfortunately, this leads to continuous increase in the number of grid points and, as a result, the computations may not be always conducted to their physical limit in time. The most promising method is the scaling of the normal coordinate, done in a manner so as to follow the profile of the boundary layer thickness in time, especially in the vicinity of the rear end point. For instance, Cebeci [17] introduces a scaled normal coordinate $\eta = y/H$, where the quantity H is defined as a function of time:

$$H \approx t^{1/2} \quad \text{for } t \leqslant 1 , \qquad H \approx \exp(t) \quad \text{for } t \geqslant 1 , \tag{7}$$

but the same limitations apply since scaling with the value of the thickness at the rear end region leads to a decrease in the number of informative grid points in the region without separation since there the thickness grows much slower with time.

In order to overcome that difficulty, the quantity H has to be not only a function of time, but also of the longitudinal coordinate, i.e., H must virtually be proportional to the boundary layer thickness which is the approach in the present paper.

As has been mentioned above, when approaching the outer edge of the boundary layer, the behavior

of the velocity is asymptotic and hence the thickness is an artificially introduced quantity needed only for the purposes of numerical treatment. Hence it can be defined quite arbitrarily. One of the ways to do that is to calculate it from the inverse of the normal gradient of the longitudinal component at $\eta = 1$. However, our experience in that direction turned out to be negative and we were faced with growing oscillations of the solution despite the absolutely stable fully implicit scheme we employed for calculating the velocity component. This setback should not be surprising since the numerical differentiation is a notoriously incorrect operation which, as a rule, increases the truncation error in order of magnitude. Moreover, that the numerically evaluated derivative is very close to zero (the asymptotic condition) and hence the errors introduced by the numerical differentiation may become an order of magnitude greater than the value sought. Stability of the algorithm was attained only after the function $H(t, x)$ was set proportional to the displacement thickness

$$\delta^*(t, x) = \int_0^\infty \left[1 - \frac{u(t, x, y)}{U_e}\right] \mathrm{d}y \,. \tag{8}$$

The typical values of the coefficient of proportionality are from the interval [6, 8], which secures the asymptotic behavior at $\eta \to 1$. Here it should be mentioned that taking the magnitude of δ^* from the previous time step does not spoil the stability.

Upon employing a scaled normal coordinate $\eta = y/H$ and introducing a new dependent variable in the place of the normal component of velocity,

$$w \equiv \frac{1}{H}\left(v - \eta \frac{\partial H}{\partial t} - \eta u \frac{\partial H}{\partial x}\right), \tag{10}$$

(2) is recast in the form

$$\frac{\partial u}{\partial t} + u \frac{\partial u}{\partial x} + w \frac{\partial u}{\partial \eta} = \frac{\partial U_e}{\partial t} + U_e \frac{\partial U_e}{\partial x} + \frac{1}{H^2} \frac{\partial^2 u}{\partial \eta^2} \,. \tag{11}$$

In turn, the equation of continuity (1) transforms into an equation for the new dependent variable

$$\frac{\partial w}{\partial \eta} = -\frac{1}{H}\left(\frac{\partial H}{\partial t} + \frac{\partial (Hu)}{\partial x}\right). \tag{12}$$

Boundary conditions (3), (4) take the form

$$u = w = 0 \quad \text{for } \eta = 0 \,, \qquad u = U_e(t, x) \quad \text{for } \eta = 1 \,, \tag{13}$$

and the initial (with respect to time) condition (5) recasts as follows:

$$u = 0 \quad \text{for } \eta = 0 \,, \qquad u = U_e \quad \text{for } \eta > 0 \,, \qquad H(t = 0, x) = \text{const.} \tag{14}$$

The boundary conditions with respect to the longitudinal coordinate (6) (the inlet and outlet conditions) are left in their original form.

3. Difference scheme

It does not pose a problem to devise an unconditionally stable difference scheme for the boundary layer equations when the sign of the longitudinal component of the velocity is positive everywhere in the region occupied by the flow. A number of difference approximations are known. As a rule they are descendants either of the Crank–Nicolson scheme or of Keller's 'box' method [22, 23] and are well documented in the literature (see, e.g., [5]). After a discretization with respect to the temporal

coordinate, the equations are recast into quasi-steady form and then solved numerically marching alongside the longitudinal coordinate x. The absolute stability of the schemes is guaranteed by the fact that the longitudinal component of velocity does not change its sign.

The situation differs drastically when a reversing zone is present in which the disturbances are convected opposite to the main flow direction. Then, in order to correctly acknowledge the convection in the difference scheme, one also has to consider the value of the velocity in the downstream vicinity of the point in which the equations are approximated. Naturally, in this case the marching methods for the steady equations become highly unstable and only the unsteady equation remains correct. One of the frequently used approximations is the so-called 'zig-zag' scheme, employed, among others, by Cebeci [13] and Wang [14]. In the regular mesh

$$\begin{aligned} &x_0 = 0\,, \quad && x_i = x_{i-1} + h_x \quad && (i = 1, 2, \ldots, I)\,, \\ &\eta_0 = 0\,, \quad && \eta_j = \eta_{j-1} + r \quad && (j = 1, 2, \ldots, J)\,, \\ &t^0 = 0\,, \quad && t^n = t^{n-1} + \tau \quad && (n = 1, 2, \ldots, N)\,, \end{aligned} \tag{15}$$

the difference approximation of the 'zig-zag' scheme has the form

$$\frac{\partial u}{\partial x} \approx \frac{u_{ij}^n - u_{i-1,j}^n + u_{ij}^{n-1} - u_{i-1,j}^{n-1}}{2h_x}\,. \tag{16}$$

For the sake of brevity, the dependence on the normal coordinate (the index j) is suppressed in the notation whenever possible.

It can be shown that the well known Courant–Friedrichs–Lewy condition is not automatically satisfied for the above approximation, especially in the case when the characteristic direction s of the operator: $\partial/\partial t + u\,\partial/\partial x$ coincides with the line s_1 shown in Fig. 1. In other words, the algorithm is stable only when the computational region of dependence contains the actual region of dependence which imposes the following limitation on the time increment:

$$\tau < -h/u \quad \text{for } u < 0\,, \tag{17}$$

i.e. the 'zig-zag' scheme is conditionally stable.

A comprehensive survey on the currently used approximations in the reversing zone is given in [5]. As an alternative to the 'zig-zag' scheme, Telionis [5] points out the scheme of Keller [24], originally implemented in [17], in which the derivatives with respect to t and x are replaced by the single Lagrangian derivative with respect to the characteristic direction s. Then

$$\frac{\partial}{\partial t} + u\frac{\partial}{\partial t} = \left.\frac{\mathrm{d}}{\mathrm{d}t}\right|_{s=\text{const}} \tag{18}$$

and when s coincides with s_1 (Fig. 1), one has

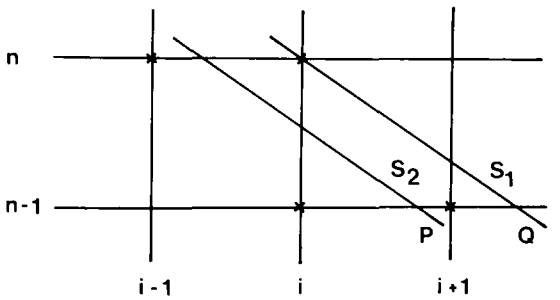

Fig. 1. The points taking part in 'zig-zag' approximation (×) and the points included in the characteristics scheme, s_1, s_2.

$$\frac{\partial}{\partial t} + u\frac{\partial}{\partial x} \approx \frac{u_i^n - u_Q^{n-1}}{\tau}. \tag{19}$$

Unlike the 'zig-zag' scheme, the Courant–Friedrichs–Lewy condition is satisfied here and the scheme is stable. As far as s_1 is a characteristic direction, then $(x_i - x_Q) = \tau u$ and therefore

$$\frac{u_i^n - u_Q^{n-1}}{\tau} = \frac{u_i^n - u_i^{n-1}}{\tau} + \frac{u_i^{n-1} - u_Q^{n-1}}{\tau} = \frac{u_i^n - u_i^{n-1}}{\tau} + u\frac{u_i^{n-1} - u_Q^{n-1}}{x_i - x_Q}. \tag{20}$$

Equation (20) shows that the approximation is rather close to the 'zig-zag' scheme provided that in the latter the local longitudinal spacing is taken to be equal to $(x_i - x_Q)$. However, to have the same spatial approximation, one needs $|x_i - x_Q| \leq h_x$, i.e., the approximation (19) is not to be taken alongside the characteristic direction s_1, but rather alongside s_2 (Fig. 1). The latter imposes the same limitations on the time increment as in the 'zig-zag' scheme.

The conclusion of the above brief review is that for separated boundary layer flows, an absolutely stable fully implicit difference scheme has not yet been used (see also reviews of Telionis [5] and Cousteix [7]).

In the present work, we make use of the method of fractional steps, namely the second scheme of Douglas and Rachford [25] (sometimes called the 'scheme of stabilizing correction' [26]). Of course, one can use also the alternating directions implicit (ADI) scheme which is of second order of approximation with respect to time but we prefer the first order accurate in time scheme of stabilizing correction because of its increased margin of stability in the non-linear case. Let us denote

$$\mathscr{A} = -u\frac{\partial}{\partial x}, \qquad \mathscr{B} = -w\frac{\partial}{\partial \eta} + \frac{1}{H^2}\frac{\partial^2}{\partial \eta^2}, \qquad \mathscr{F} = \frac{\partial U_e}{\partial t} + U_e\frac{\partial U_e}{\partial x}. \tag{21}$$

Then the stabilizing correction scheme reads

$$\frac{\tilde{u} - u^{n-1}}{\tau} = A\tilde{u} + Bu^{n-1} + f_i^n, \tag{22}$$

$$\frac{u^n - \tilde{u}}{\tau} = B(u^n - u^{n-1}), \tag{23}$$

where A, B and f stand for the difference approximations of the operators $\mathscr{A}$, $\mathscr{B}$ and function $\mathscr{F}$, respectively.

The approximation with respect to time can be assessed after excluding the half time-step variable u (see [26]), namely

$$(E - \tau A)(E - \tau B)u^n = (E + \tau B)u^{n-1} - (E - \tau A)\tau Bu^{n-1} + f_i^n, \tag{24}$$

where E is the identify operator. After obvious manipulations, we obtain

$$(E + \tau^2 AB)\frac{u^n - u^{n-1}}{\tau} = (A + B)u^n. \tag{25}$$

It is easily seen now that the scheme possesses so-called 'full approximation' [26], in the sense that when $u^{n-1} \to u^n$ it gives for the steady equation approximation that is independent of the magnitude of time increment τ. The latter is of crucial importance for application to the stationary boundary layers flows. Here it should be mentioned that not all schemes of splitting type possess the property of full approximation [26].

We show here that when the non-linear coefficients of operators $\mathscr{A}$ and $\mathscr{B}$ are thought of as known

(the method of 'frozen' coefficients), the scheme is unconditionally stable. The differential operator $\mathscr{A}$ is oblique and $\mathscr{B}$ is negatively definite (see the definitions in (21)), i.e.,

$$(\varphi, A\varphi) = 0\,, \qquad (\varphi, B\varphi) \leqslant -\gamma \|\varphi\|\,, \quad \gamma > 0\,. \tag{26}$$

Then one has

$$\|E - \tau A\| = 1\,, \qquad \|E - \tau B\| \geqslant 1\,, \qquad \|(E + \tau^2 AB)\| \geqslant 1\,,$$

and therefore

$$\|(E - \tau A)(E - \tau B)\|^{-1} \leqslant 1 \quad \text{and} \quad \|(E + \tau^2 AB)\|^{-1} \leqslant 1\,, \tag{27}$$

which for the differential form of the splitting type scheme is a sufficient condition for stability. The said property is also retained for the difference form provided that, after proper linearization, a conservative differencing for the set functions that secures the properties (26) is employed (see, e.g., [27, 28]). Therefore the scheme is stable. The most consistent way to treat the non-linearity is to employ Newton's quasi-linearization securing second order in time approximation of the non-linear terms. This is not done here because the scheme is first order in time due to splitting. Thus, the simplest way for linearization of A and B, the above mentioned 'frozen' coefficients, is chosen. Then the first half time step, (22), adopts the form

$$\frac{\tilde{u}_{i,j} - u_{i,j}^{n-1}}{\tau} + u_{i,j}^{n-1} \left.\frac{\delta \tilde{u}}{\delta x}\right|_{i,j} = \Phi_{i,j}\,, \tag{28}$$

where $\Phi_{i,j}$ is a known set function and $\delta\tilde{u}/\delta x$ stands for the difference approximation of the first derivative. Here it is to be pointed out that for (28) a fully implicit approximation can be devised that is independent of the sign of the longitudinal component of velocity. Hence, the region of dependence is limited only by the region of flow. The latter imposes the limitation that, if the boundary layer incorporates a reversing zone, the latter is to be entirely imbedded into the computational domain.

Speaking about the approximation of the longitudinal derivatives in (28), one can say that unconditionally stable difference schemes can be constructed with both first and second order of approximation, provided the respective conservative differencing is applied for $\delta/\delta x$ (see, for instance, [27, pp. 128–129; 28]). The first order schemes employ, as a rule, upwind differences and exhibit considerable scheme viscosity (artificial diffusiveness). The latter is not necessarily an undesirable property in a scheme because it also helps to damp the non-physical oscillations that are being amplified by the non-linear terms. It is preferable to start the calculations (as is done in [29]) with a first order scheme and only after the limitations of the numerical algorithm are revealed and the regions for parameters in which stable calculations are possible are found. Then one could repeat the computations with the second order scheme.

Following this general notion, in the present paper two different schemes are proposed and the following difference approximations are employed: for the first order scheme, the upwind differences

$$\frac{\delta\tilde{u}}{\delta x} = \begin{cases} [\tilde{u}_{i,j} - \tilde{u}_{i-1,j}]/h_x\,, & \text{if } u_{i,j}^{n-1} \geqslant 0\,, \\ [\tilde{u}_{i+1,j} - \tilde{u}_{i,j}]/h_x\,, & \text{otherwise}\,, \end{cases} \tag{29}$$

and for the second order scheme, the central differences

$$\frac{\delta\tilde{u}}{\delta x} = \frac{\tilde{u}_{i+1,j} - \tilde{u}_{i-1,j}}{h_x}\,. \tag{30}$$

Concerning the three-point second order scheme (30) for the first derivative, the following features should be mentioned:

(1) The simple Thomas algorithm [27] cannot be used in general but rather a Gaussian elimination with pivoting is to be applied when solving the resulting three-diagonal algebraic system, since the main diagonal dominates only if the spacing and time increment are related in order to satisfy the condition $\tau u/h < 1$ (which is nothing else but the Courant–Friedrichs–Lewy condition).

(2) The three-point approximation requires two boundary conditions. In the case of flow around blunt bodies (including the case of a cylinder moving from rest), the second condition stems from the symmetry condition at the rear end stagnation point. In those cases where a second boundary condition cannot be deduced from physical considerations (e.g., for bodies with sharp rear ends), one has to employ the two-point difference approximation in the last mesh point of the longitudinal direction.

When approximating the operators from the second half time step, one can employ either the box method of [23] or the central difference scheme. The differences between them show up only when a non-uniform mesh is employed, namely

$$\eta_0 = 0\,, \qquad \eta_j = \eta_{j-1} + r_j \quad (j = 1, 2, \ldots, J)\,. \tag{31}$$

In this case, the box method gives a scheme of second order of approximation $O[\max(r_j^2)]$, but it is implemented as a vector three-diagonal system.

In the present paper, the difference scheme is used (equivalent to the central differences scheme on uniform mesh) and the derivatives are approximated as follows:

$$\frac{\delta u}{\delta \eta} = \frac{u_{j+1} - u_{j-1}}{r_j + r_{j+1}}\,, \tag{32}$$

$$\frac{\delta^2 u}{\delta \eta^2} = \frac{2}{r_j + r_{j+1}}\left[\frac{u_{j+1} - u_j}{r_j} - \frac{u_j - u_{j-1}}{r_{j-1}}\right]. \tag{33}$$

In this case, the order of approximation is $O[\max(r_j r_{j-1}, r_j - r_{j-1})]$. Note that within the said order, the approximation (32) coincides with the standard approximation for a first derivative on a non-uniform mesh. The scheme (32) has some advantages connected with its conservation properties. It is obvious then that the requirement of adequate approximation is that the variation of mesh spacing r_j with the index j must not be very strong. This is a limitation, of course, but it is paid off by the fact that one is faced now with a plain three-diagonal system for a scalar unknown.

For the continuity equation (12), we employ the following standard scheme with a second order of approximation with respect to both spatial variables:

$$\frac{w^n_{i,j+1} - w^n_{ij}}{r_j} = -\frac{1}{H^n_j}\left[\frac{H^n_i - H^{n-1}_i}{\tau} + \frac{u^n_{i+1,j+1}H^n_{i+1} - u^n_{i-1,j+1}H^n_{i-1}}{4h_x} + \frac{u^n_{i+1,j}H^n_{i+1} - u^n_{i-1,j}H^n_{i-1}}{4h_x}\right]. \tag{34}$$

4. Grid pattern

The adequate non-uniform distribution of the grid points in the normal direction is of crucial importance for the performance of the numerical algorithm. The grid pattern is to be consistent with the intrinsic features of the problem, such as the presence of non-uniform gradients of the required variables. The best way is to devise a rule for tuning the mesh to the gradients (see, for instance, [30]) adaptively during the calculations (for a comprehensive survey see, e.g., [31, 32]). At this stage, however, we are not prepared for such a general approach to the mesh problem and hence we rely on a

particular analytical law for the grid distribution in the normal direction which is selected on the basis of general considerations on the behavior of variables in a separated boundary layer.

In a separated unsteady boundary layer, two regions are formed [20, 33]. The first one is adjacent to the rigid wall and evolves slowly in time. In that region, the longitudinal component of velocity falls sharply from zero to its minimal (the largest negative) value and the velocity gradient is considerable there. The thickening of the boundary layer, however, is due chiefly to the development of the second (outer) region in which the longitudinal component rises to its asymptotic value from the ideal flow. The gradient there adopts low and moderate magnitudes. Thus, the transverse distribution of the gradients in the separated laminar boundary layer resembles, in a sense, the structure of a turbulent boundary layer with the first region playing the role of a viscous sub-layer.

Guided by the above analogy, we take the following law for the distribution of a mesh in the normal direction:

$$\eta_j = \frac{1}{\omega}\left[\frac{j-1}{J-1} + 0.4\right]\left\{\exp\left[\frac{j-1}{J-1}\ln\frac{\omega+1.4}{1.4}\right] - 1\right\}, \tag{35}$$

where ω is a parameter responsible for deviation of the grid pattern from the uniform shape. As mentioned above, the accuracy of the scheme is $O[\max(r_j r_{j-1}, r_j - r_{j-1})]$. A uniform approximation will be present if and only if $\max(r_j - r_{j-1})$ is of order of magnitude $\max(r_j r_{j-1})$. Values of ω for which $\max(r_j r_{j-1}) \approx \max(r_j - r_{j-1})$ and the mesh is sufficiently non-uniform are from the interval [50, 100].

5. Numerical tests and verifications

In order to assess the approximation of the proposed scheme and the performance of the algorithm, a number of numerical experiments have been conducted. We began with the upwind differences in the longitudinal direction according to (29). The time evolution of the computed quantities was stable and no oscillations were present. That encouraged us to increase the order of approximation in the longitudinal direction according to (30). The calculations remained unequivocally stable and monotonic.

The second group of numerical experiments were aimed at assessing the influence of the normalwise grid distribution. Acknowledging that for a circular cylinder the relation $x = 2\pi\theta/180°$ is valid, we refer in what follows to the 'longitudinal' angle θ rather than to the longitudinal coordinate x. Respectively, h_θ stands for the spacing related to the angle. In order to minimize the computational time, a rougher spacing in longitudinal direction with 73 points ($h_x = 2\pi/72$, $h_\theta = 2.5°$) and a relatively large time increment $\tau = 0.04$ were used. In the normal direction, we took consecutively 26, 51 and 101 mesh points and set the grid parameter $\omega = 100$. The comparisons presented in Table 1 are for the displacement thickness which is one of the most spoiled quantities for the problem under consideration, especially in the interval $[100° \leq \theta \leq 135°]$, where for larger times, non-monotonic behavior develops. It is seen that the results obtained with 51 and 101 points in the normal direction differ less than by 0.5%. This accuracy is acceptable and hence the chief portion of the calculations to be mentioned below are conducted with 51 points. For the sake of comparison it must be mentioned that Cebeci [10, 17] employs meshes with 301 and 161 points, respectively. The good accuracy attained in the present work on rougher meshes, we attribute to the adequate choice of the non-uniform grid pattern.

Table 1
Displacement thickness for $t = 2.8$, $\tau = 0.04$, $I = 73$

J	$\theta = 105°$	$\theta = 110°$	$\theta = 115°$	$\theta = 120°$	$\theta = 125°$	$\theta = 130°$	$\theta = 135°$
101	2.075	3.001	7.204	9.547	9.094	9.198	9.374
51	2.077	3.012	7.237	9.590	9.133	9.238	9.412
26	2.087	3.055	7.575	9.752	9.378	9.443	9.547

Table 2
Friction coefficient for $t = 2.8$, $J = 51$

τ, I	$\theta = 30°$	$\theta = 60°$	$\theta = 90°$	$\theta = 120°$	$\theta = 150°$
$\tau = 0.04$, $I = 289$	0.5779	0.7966	0.4783	−0.5070	−0.4871
$\tau = 0.02$, $I = 73$	0.5778	0.7964	0.4776	−0.5087	−0.4891

The third main set of experiments reveal the dependence of the results on the particular values of the mesh parameters τ and h_θ.

An interesting observation is that the flow in the immediate vicinity of the wall depends insignificantly on these parameters of the difference scheme. This conclusion is supported by the results obtained with different mesh size for the skin friction coefficient presented in Table 2 for the critical moment of time $t = 2.8$. It is seen that those results differ by less than 0.5%. This allows us to present further results for the local skin friction coefficient without explicitly mentioning the particular size of the mesh on which those results are obtained.

Unlike the case of the skin friction coefficient, the dependence of the displacement thickness and displacement velocity $v_\infty = \partial(\delta^* U_e)/\partial x$ on the mesh parameters turns out to be significant. A quantitative feeling for the dependence is shown in Fig. 2(a,b) where the functions of the longitudinal coordinate are plotted for the most volatile interval $[110° \leqslant \theta \leqslant 135°]$ and for a sufficiently large value of time – $t = 2.8$. It is seen that the values in the immediate vicinity of the detachment point are especially sensitive to the mesh parameters, at the time when the rest of the values are virtually not affected from the change in the mesh parameters. The value of time increment τ affects only the longitudinal localization of the displacement thickness maximum (compare lines 1 and 3) without influencing the gradient of that quantity. Respectively, refining the longitudinal resolution (compare curves 2 and 3) results in an increase in the thickness gradient. The magnitude of $\max \delta^*$ is predicted reasonably well and the curves for the displacement thickness are quite close hence allowing us to conclude that the proposed scheme is accurate enough. It is seen that the present result are smooth, which is not the case with the results of Henkes and Veldman [18] for $t = 2.85$.

A similar conclusion about the correctness of the results obtained can be drawn from the calculated displacement velocity v_∞. The velocity is obtained by differentiation of the displacement thickness and the eventual errors are accordingly amplified. Here must be mentioned the measures taken in the present work for securing good approximation for the displacement velocity. As far as the approximation with respect to the longitudinal coordinate x is at most of second order (or even in some cases of

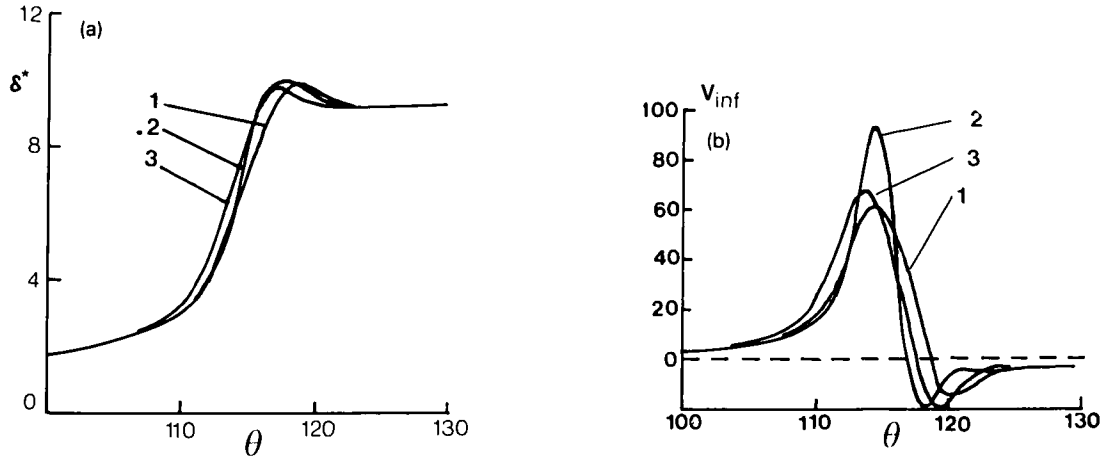

Fig. 2. Sensitivity of the computed characteristics to specific values of longitudinal spacing and time increment: (1) $h_\theta = 2.5°$, $\tau = 0.04$; (2) $h_\theta = 1.25°$, $\tau = 0.04$; (3) $h_\theta = 2.5°$, $\tau = 0.02$. (a) Displacement thickness of the boundary layer; (b) displacement velocity.

first order), the straightforward numerical differentiation of the displacement thickness with respect to x will result in decreasing the approximation to first or even zeroth order. In order not to lower the accuracy, we use a third order spline interpolation for the displacement thickness which gives a second order approximation for the first derivative. Results depicted in Fig. 2(a) are obtained by means of the said spline interpolation.

6. Result and comparisons

After the difference scheme and the algorithm have been properly verified, we turn to investigating the separation itself. Our results show (see Fig. 2(a)) that for $t \geq 2.5$, the displacement thickness δ^* grows quickly and for approximately $t \approx 2.8$ a distinct local maximum is formed. These findings are in good agreement with the predictions of Van Dommelen and Shen [12].

As has already been mentioned, the displacement velocity is more suited for quantitative assessment of the separation as it is more sensitive. According to Van Dommelen and Shen [11, 12], $\max(-\partial u/\partial x) \to \infty$ for $t \to 3$ proportionally to $(3-t)^{-1.75}$. It can be shown that the displacement velocity is a proper indicator for that type of behavior (see, e.g., [15]), since it grows according to the formula $v_\infty \approx (3-t)^{-1.75}$. On the other hand, it is well known that the value of v_∞ is a measure for the influence of the boundary layer on the outer potential flow. In the classical theory of boundary layers, when no separation is expected, the displacement velocity behaves as $v_\infty \approx O(\mathrm{Re}^{-1/2})$. Therefore, the above suggested behavior of v_∞ speaks of singularity whose occurrence disables the classical theory. For this reason the displacement velocity v_∞ turns out to be one of the most important characteristics of the unsteady boundary layer. Figure 2(b) hints that in order to prove that $v_\infty \to \infty$ for $t \to t_s$, one needs a very fine longitudinal resolution of the mesh (very small h_θ). It is instructive, therefore, to trace the variation in the solution with decreasing spacing h_θ. In Fig. 3 are compiled the results for the maximal value of the displacement velocity obtained on three different meshes with the number of points in the longitudinal direction 73 ($h_\theta = 2.5°$), 145 ($h_\theta = 1.25°$), 289 ($h_\theta = 0.625°$), respectively. In the logarithmic scales adopted in Fig. 3, the tendency of the computed curve to approach a line when $h_\theta \to 0$ is easily seen. Our results give the slope of the line = 1.7414. The respective value of [12] is 1.75. The results of [15, 16] are also very close to this value.

Another important characteristic of the boundary layer flow whose behavior in the separation zone is instructive, is the local skin friction coefficient. Van Dommelen and Shen [12] state that this quantity exhibits regular behavior when $t \to t_s$ and hence cannot be used as an indicator of the occurrence of

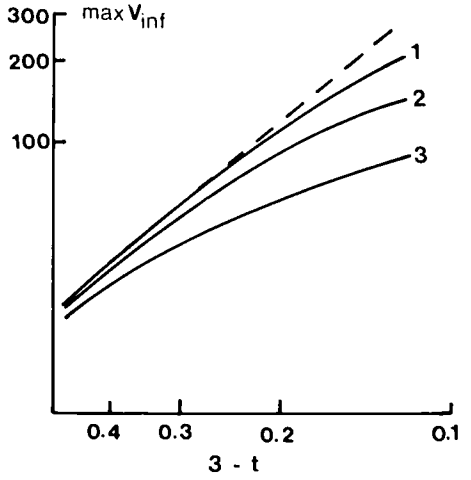

Fig. 3. Evolution of the displacement velocity when $t \to 3$: expected behavior of the exact solution according to $\ln V_{inf} = -1.7414 \ln(3-t) + 1.9597$. (1) $h_\theta = 0.625°$; (2) $h_\theta = 1.25°$; (3) $h_\theta = 2.5°$.

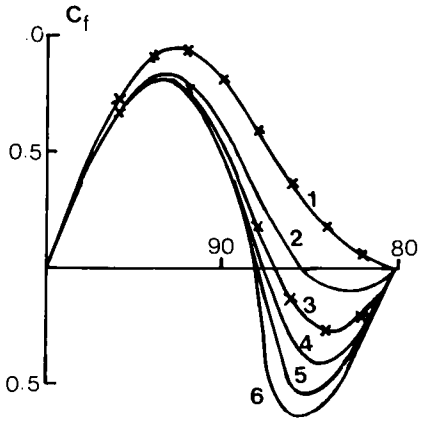

Fig. 4. Evolution of the local friction coefficient with time: ×, asymptotic results of [34]; —, present numerical results: (1) $t = 0.5$; (2) $t = 1.0$; (3) $t = 1.5$; (4) $t = 2.0$; (5) $t = 2.5$; (6) $t = 3.0$.

unsteady singularity. It is important to compare it with the results of other authors in order to have an additional verification of the performance of the algorithm. This is done in Fig. 4 where the analytic results of Bar-Lev and Yang [34] are plotted.

Following Blasius [35], most authors report data concerning the position on the wall of the point with zero skin friction as a function of time which characterizes adequately the evolution of the separation zone. It is believed now that the point of zero skin friction occurs initially for $t \approx 0.644$ [8, 11, 15]. The present results (Fig. 5) are not only in very good agreement with that value but also with the asymptotic formula of [34] for the entire time interval. Some slight deviations (less than 1°) are observed only for $t \approx 3$ where the flow conditions are indeed too harsh to conduct a numerical investigation. Here it must be mentioned that the same good agreement is reported by Van Dommelen and Shen [11] for the computations with the Lagrangian scheme.

In certain numerical schemes for investigating the boundary layer flow around blunt bodies, similar variables and coordinates as in asymptotic solutions are employed [10, 11, 13] which allows one to use the similar solutions as initial (inlet) or boundary (outlet) conditions for the numerical scheme. In the present paper, such an eclectic approach is avoided and this gives another opportunity to check the accuracy of the computations by comparing the latter with these similar solutions. In Fig. 6(a,b) are plotted the values of skin friction in the leading and rear end regions, respectively, after being rendered

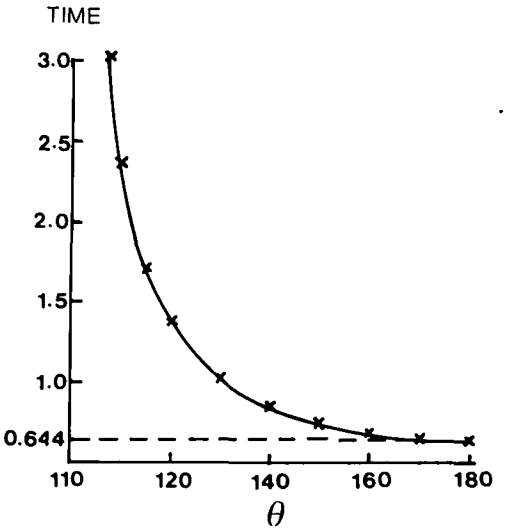

Fig. 5. Trajectory of the point of zero skin friction: ×, asymptotic results of [34]; —, present numerical results.

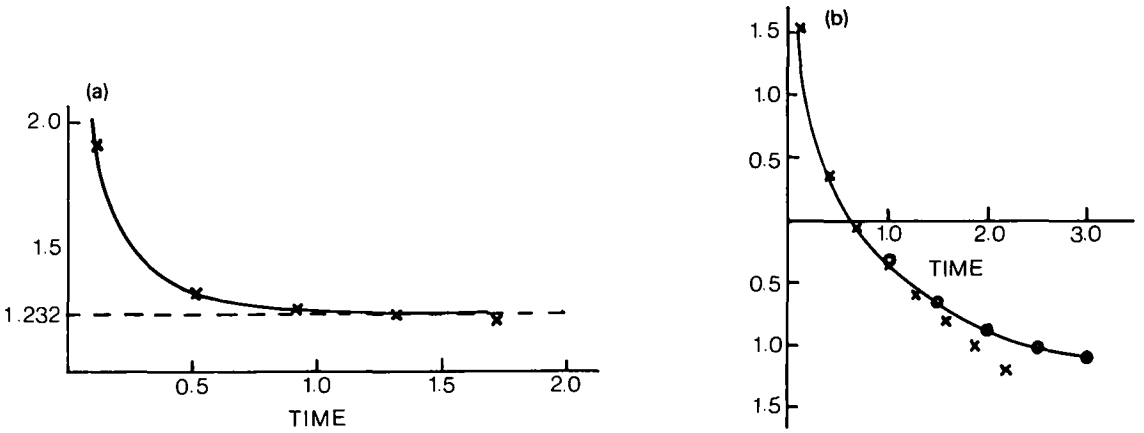

Fig. 6. The skin friction coefficient in terms of local similar variables: ×, asymptotic results of [34]; ○, numerical results of [15, 21, 36]; —, present numerical results. (a) Leading end point; (b) rear end point rendered.

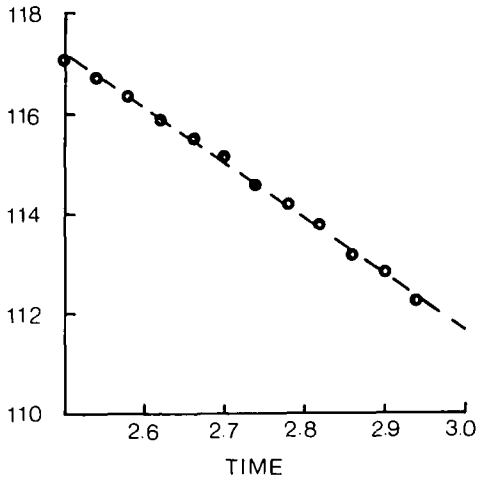

Fig. 7. Trajectory of the point of maximum displacement velocity: —, the linear approximation $\theta = 145.06° - 11.135°t$; O, present numerical results.

similar variables. In both cases, the results are in good agreement with those of [10, 11, 34]. In Fig. 6(b), the numerical results of [15, 21, 36] are presented in a generalized form because they coincide among themselves up to the third digit. The agreement is excellent, which gives additional support for the main claim of the present work that a properly devised difference scheme in Eulerian variables can bring the same results as the schemes in Lagrangian variables.

Another important feature of the unsteady separation observed in [12, 16] is that the point of singularity of the solution moves alongside the wall in the opposite direction to the main flow with a constant velocity. Our results are plotted in Fig. 7 and they lie virtually on a straight line which for $t = 3$ gives $\theta \approx 111.6°$. Let us note here that Van Dommelen and Shen [21] report $\theta \approx 111°$ for that value.

7. Concluding remarks

In the present paper, a fully implicit unconditionally stable Eulerian difference scheme for the numerical investigation of unsteady boundary layers is developed. The scheme performs equally well when a separation occurs. A number of numerical tests and verifications are conducted in order to outline the limits of application of the algorithm. Comparisons with other numerical results in Lagrangian variables and with asymptotic analytical solutions are presented. The agreement is good and the conclusion is that the observed discrepancy in the literature between the Lagrangian and Eulerian schemes is not principal and predictions of the latter can be brought closer to the former provided implicit differencing is employed.

The results support the findings of the authors using Lagrangian schemes that a singularity which is not of Goldstein type develops for finite times $t_s \approx 3$. Different calculations of physical significance are presented graphically.

Acknowledgment

The authors wish to thank Professor Riley for making his paper available to us at the stage of galley proofs. This work is supported in part by Grant 741 from the Ministry of Culture, Science and Education of Bulgaria.

References

[1] S. Goldstein, On laminar boundary layer flow near a position of separation, Quart. J. Mech. Appl. Math. 1 (1948) 43–69.
[2] Ta Phuoc Loc, Numerical analysis of unsteady secondary vortices generated by an impulsively started circular cylinder, J. Fluid Mech. 100 (1980) 111–128.
[3] Ta Phuoc Loc and R. Bouard, Numerical solution of the early stage of the unsteady viscous flow around a circular cylinder: A comparison with experimental visualisation and measurements, J. Fluid Mech. 160 (1985) 93–117.
[4] R. Bouard and M. Coutanceau, The early stage of development of the wake behind an impulsively started cylinder for $40 < Re < 10^4$, J. Fluid Mech. 101 (1980) 583–607.
[5] D.P. Telionis, Unsteady Viscous Flows (Springer, Berlin, 1981) 408 p.
[6] J.W. Elliot, S.J. Cowley and F.T. Smith, Breakdown of boundary layers: (i) on moving surface; (ii) in semi-similar unsteady flow; (iii) in fully unsteady flow, Geophys. Astrophys. Fluid Dynam. 25 (1983) 77–138.
[7] J. Cousteix, Three-dimensional and unsteady boundary layer computations, Ann. Rev. Fluid Mech. 18 (1986) 173–196.
[8] W.M. Collins and S.C.R. Dennis, The initial flow past an impulsively started cylinder, Quart. J. Mech. Appl. Math. 26 (1973) 53–75.
[9] D.P. Telionis and D.T. Tsahalis, Unsteady laminar separation over impulsively moved cylinders, Acta Astronautica 1 (1974) 1487–1505.
[10] T. Cebeci, The laminar boundary layer on a circular cylinder started impulsively from rest, J. Comput. Phys. 31 (1979) 153–172.
[11] L.L. van Dommelen and S.F. Shen, The spontaneous generation of the singularity in a separating laminar boundary layer, J. Comput. Phys. 38 (1980) 125–140.
[12] L.L. van Dommelen and S.F. Shen, The genesis of separation, in: T. Cebeci, ed., Numerical and Physical Aspects of Aerodynamic Flows (Springer, Berlin, 1982) 293–364.
[13] T. Cebeci, Unsteady separation, in: T. Cebeci, ed., Numerical and Physical Aspect of Aerodynamic Flows (Springer, Berlin, 1982) 265–277.
[14] K.C. Wang, On the current controversy about unsteady separation, in: T. Cebeci, ed., Numerical and Physical Aspects of Aerodynamic Flows (Springer, Berlin, 1982) 279–291.
[15] S.J. Cowley, Computer extension and analytic continuation of Blasius' expansion for impulsive flow past a circular cylinder, J. Fluid Mech. 135 (1983) 389-405.
[16] D.B. Ingham, Unsteady separation, J. Comput. Phys. 53 (1984) 90–99.
[17] T. Cebeci, Unsteady boundary layers with an intelligent numerical scheme, J. Fluid Mech. 163 (1986) 129–140.
[18] R.A.W.M. Henkes and A.E.P. Veldman, On the breakdown of the steady and unsteady interacting boundary-layer description, J. Fluid Mech. 179 (1987) 513–529.
[19] N. Riley and R. Vasanta, Unsteady high-Reynolds number flows, J. Fluid Mech. 205 (1989) 243–263.
[20] A.J. Robins and J.A. Howarth, Boundary-layer development at a two-dimensional rear stagnation point, J. Fluid Mech. 56 (1972) 161–172.
[21] L.L. van Dommelen and S.F. Shen, The flow at a rear stagnation point is eventually determined by exponentially small values of the velocity, J. Fluid Mech. 157 (1985) 1–16.
[22] H.B. Keller, Accurate difference methods for linear ordinary differential systems subject to linear constraints, SIAM J. Numer. Anal. 6 (1969) 8–30.
[23] H.B. Keller, Accurate difference methods for nonlinear two-point boundary value problems. SIAM J. Numer. Anal. 11 (1974) 305–320.
[24] H.B. Keller, Numerical Methods in boundary-layer theory, Ann. Rev Fluid Mech. 10 (1978) 417–433.
[25] J. Douglas and H.H. Rachford, On the numerical solution of heat conduction problems in two and three space variables, Trans. Amer. Math. Soc. 82 (1956) 421–439.
[26] N.N. Yanenko, Method of Fractional Steps (Gordon and Breach, London, 1971).
[27] P.J. Roache, Computational Fluid Dynamics (Hermosa, 1972).
[28] G.I. Marchuk, Methods of Computational Mathematics (Nauka - Siberian Division, Novosibirsk, 1973) (in Russian).
[29] I. Tzankov and C. Christov, On the numerical treatment of separated unsteady boundary layers, Proc. 15th Jubilee Session of the Scientific and Methodological Seminar on Ship Hydrodynamics, Bulgarian Ship Hydrodynamics Center, Varna (1986) Vol. 3, Paper No. 21.
[30] C.I. Christov, Orthogonal coordinate meshes with manageable Jacobian, in: J.F. Thompson, ed., Numerical Grid Generation (Elsevier, Amsterdam, 1982) 885–894.
[31] J.F. Thompson, Grid generation techniques in computational dynamics, AIAA J. 22 (1984) 1505–1523.
[32] P. Eiseman, Grid generation for solution of partial differential equations, ICASE Report No 87-57, 1987.
[33] I. Proudman and K. Johnson, Boundary-layer growth near a rear stagnation point, J. Fluid Mech. 12 (1962) 161–168.
[34] M. Bar-Lev and H.T. Yang, Initial flow field over an impulsively started circular cylinder, J. Fluid Mech. 72 (1975) 625–647.
[35] H. Blasius, Grenzschichten in Flussigkeiten mit kleiner Reibung, Z. Angew. Math. Phys. 56 (1908) 1–37.
[36] M.J. Hommel, The laminar unsteady flow of a viscous fluid away from a plane stagnation point, J. Fluid Mech. 132 (1983) 407–416.